



Pharmacophore Screening and Docking studies of AMPA Receptor Implicated in Alzheimer's disease with Some CNS Acting Phytocompounds from Selected Ayurvedic Medicinal Plants

Preenon Bagchi^{1,2,†}, Anuradha M¹, Ajit Kar^{2,3}

ABSTRACT

Neuro-degeneration including dementia in Alzheimer's disease (AD) is a global alarming problem. AD accounts for 60 to 80 percent of dementia cases. AMPA (alpha-amino-3-hydroxy-5-methyl-4-isoxazole propionic acid) receptors are the main contributors of excitatory neurotransmission, mediating the fast, rapidly desensitizing excitation of many synapses, and are involved in the early response to glutamate in the synaptic space. The gene receptor AMPA responsible for AD is taken for this work. In the present study phyto-compounds from Ayurvedic Medicinal plants like *Centella asiatica*, *Bacopa monnieri*, *Convolvulus pluricaulis*, *Mucuna pruriens*, *Ocimum sanctum*, *Tinospora cordifolia*, *Curcuma longa*, *Nardostachys jatamansi* are among others used. The active components of the plants are taken and pharmacophore screening along with docking studies are performed against AMPA receptor in silico. The docking scores are noted for further in-vitro receptor-ligand binding assay studies. The selected phytocompounds were screened against AMPA receptor. Again, ADME (drug-like properties) was determined for the shortlisted ligands. Based on virtual screening, shortlisted ligands selected were Quercetin dihydrate and Asiatic acid.

Keywords:

Alzheimer's disease (AD), AMPA, Modeling, Ramachandran plot, Pharmacophore, docking, ADME

Introduction

Since ages various medicinal plants are part & parcel of major populations of India & other South East Asian countries. For the management of different neuro-degenerative diseases (Alzheimer's, parkinsonism, obsessive compulsive disorder (OCD), ageing related metabolic disorders and stress-induced dysfunctions, mania, depression, acute &

chronic cases of dementia, etc.) - where chemical & synthetic drugs are not fully effective, different phytomedicinal compounds (phytochemicals from herbal sources) may be successfully utilized with minimum or without side effects even for long term therapy. For the management of different mental & neuronal disorders there is tremendous scope of discovery of specific phytocompounds from medicinal plants. The

¹Padmashree Institute of Management and Sciences, Bangalore, India

²Sarvasumana Association, Bangalore, India

³Satsang Herbal Research Laboratory, Deoghar, India

[†]Author for correspondence: Preenon Bagchi, Padmashree Institute of Management and Sciences, Bangalore, India, email: prithish.bagchi@gmail.com

binding affinity of specific phytochemicals with the gene-products (i.e., specific proteins) of the above disorders using bioinformatic softwares can prove effective for future drug discovery using these phytochemicals [1-3].

Alzheimer's disease (AD) is a type of dementia that causes problems with memory, thinking and behavior; symptoms usually develop slowly and get worse over time, becoming severe enough that it interferes with daily tasks. The greatest known and studied risk factor is increasing age, and the majority of people with AD are 65 and older. AD is a progressive disease, where dementia symptoms gradually worsen over a number of years and in its early stages, memory loss is mild, but with late-stage AD, individuals lose the ability to carry on a conversation and respond to their environment. Now, there is a worldwide effort under way to find better ways to treat and fight the disease and to delay its onset. Dementia is the loss of cognitive functioning—thinking, remembering, including reasoning—and behavioral abilities to such an extent that it interferes with a person's daily life and activities and it ranges in severity from the mildest stage, when it is just beginning to affect a person's functioning, to the most severe stage, when the person must depend completely on others for basic activities of daily living [4-6].

AD is named after Dr. Alois Alzheimer. In 1906, Dr. Alzheimer noticed changes in the brain tissue of a woman who had died of an unusual mental illness; her symptoms included memory loss, language problems, and unpredictable behavior. After she died, he examined her brain and found many abnormal clumps (also called amyloid plaques) and tangled bundles of fibers (now called neurofibrillary, or tau, tangles); these plaques and tangles in the brain are still considered some of the main features of AD. Another feature is the loss of connections between nerve cells, the neurons in the brain. Neurons transmit messages between different parts of the brain, and from the brain to muscles and organs in the body. Abnormal deposits of proteins form amyloid plaques and tau tangles are found throughout the brain. Once-healthy neurons stop functioning; they lose connections with other neurons and ultimately die. The damage initially appears to take place in the hippocampus, the part of the brain essential in forming memories, and as more neurons die, additional parts of the brain are affected, and they begin to shrink. By the time the final stage of AD has widespread, and brain tissue has shrunk significantly [6-8].

Materials & Methods

For the present study the following medicinal plants have been selected to study the scope & activity of different phyto-compounds using bioinformatic parameter, these are *Convolvulus pluricaulis*, *Morus alba*, *Bacopa monnieri*, *Phyllanthus emblica*, *Gymnema sylvestre*, *Eclipta alba*, *Glycyrrhiza glabra*, *Gymnema sylvestre*, *Vitex negundo*, *Picrorhiza kurrooa*, *Azadirachta indica*, *Ruta graveolens*, *Trigonella foenum-graecum*, *Momordica charantia*, *Vitex negundo*, *Terminalia arjuna*, *Centella asiatica*, *Bacopa monnieri*, *Acacia nilotica*, *Terminalia chebula*, *Coffea arabica*, *Sutherlandia frutescens/Bougainvillea spectabilis*, *Phyllanthus emblica*.

Mutated mammalian AMPA implicated as factor causing AD were retrieved from the National Centre for Biotechnology Information (NCBI); templates as retrieved from BLAST were downloaded from PDB. The 3D structure of AMPA was determined by homology modelling. The 3D structures of phytocompounds (from Ayurvedic herbs) were retrieved from various databases. The pharmacophore hypothesis was generated for the existing ligands and the phytocompounds were screened against the generated pharmacophoric hypothesis. Ligands were shortlisted based on their fitness score. Mutations in the AMPA (α -amino-3-hydroxy-5-methyl-4-isoxazolepropionic acid) are noted as causal factors for many CNS disorders are used in this work [7-9].

■ AMPA receptor

The α -amino-3-hydroxy-5-methyl-4-isoxazolepropionic acid receptor (also known as AMPA receptor, AMPAR or quisqualate receptor) is a non-NMDA-type ionotropic transmembrane receptor for glutamate that mediates fast synaptic transmission in the central nervous system (CNS) [9-11]. Its name is derived from its ability to be activated by the artificial glutamate analog AMPA. The receptor was first named the "quisqualate receptor" by Watkins and colleagues after a naturally occurring agonist quisqualate and was only later given the label "AMPA receptor" after the selective agonist developed by Honore et al. [10] at the Royal Danish School of Pharmacy in Copenhagen. AMPARs are found in many parts of the brain and are the most commonly found receptor in the nervous system. The AMPA receptor GluA2 (GluR2) tetramer was the first glutamate receptor ion channel to be crystallized. The idea is that AMPARs are trafficked from the dendrite

into the synapse and incorporated through some series of signaling cascades. AMPA receptors are responsible for the bulk of fast excitatory synaptic transmission throughout the CNS and their modulation is the ultimate mechanism that underlies much of the plasticity of excitatory transmission that is expressed in the brain [9-12].

In this work the 3D structure of the mutated AMPA receptor responsible for AD and related CNS disorders is modeled & virtually screened against the phytocompounds given.

■ Methodology

The 3D structure of the AMPA receptor is modelled using modeler software [13]. The AMPA receptor amino acid sequence is downloaded from NCBI; its homologous templates were selected by BLAST. The receptor and their corresponding templates were submitted to modeler software to model their 3D structure. Using Rampage ramachandran plot server the models generated by modeler are analyzed and the best model is selected.

■ Model quality assessment

Sali and Blundell [13] generated five models. Using Rampage Ramachandran Plot Server, (this stereochemical check was applied to verify if the ϕ and ψ dihedral angles were in available regions of the Ramachandran plot) the best protein model was selected [14].

Phyto-compounds from traditional ayurvedic herbs

■ Ligand preparation

The 3d structures of the above phyto-compounds were downloaded from PubChem, a database of chemical molecules maintained by the NCBI and various other online databases.

■ Generating phase database

Now using Application→Phase→Generate Phase Database module of Maestro software phase database of the phyto-compounds was done [2,15-17].

■ Selection of ligands for AMPA receptor

Structure-based pharmacophore model is a novel procedure for generating energy-optimized pharmacophore (e-pharmacophores) is based on mapping of the energetic items from the Glide XP scoring function onto atom centers. This was selected by mining the regular features of the three-dimensional structure of AMPA receptor interacting with the known. Phores were selected

in the 3D structure of the AMPA receptor at the interaction sites with the known ligands. AMPA receptor with the structural phore information was loaded in the Maestro workspace. Beginning with a ligand-receptor complex structure, we improve the ligand pose, compute the Glide XP scoring items, and map the energies onto atoms. Then, pharmacophore sites were produced, and the Glide XP energies from the atoms that encompass each pharmacophore site were summed. The sites were then graded based on these energies, and the most positive sites were selected for the pharmacophore hypothesis. Finally, these e-pharmacophores were used as queries for virtual screening [2,15-17].

■ Docking

Docking was performed by Docking server by selecting the best model (model 3) with the ligand selected by pharmacophore modeling, colchicine, to get the docked structure [18].

■ ADME screening

ADME is an abbreviation in pharmacology and pharmacokinetics for absorption, distribution, metabolism, and excretion. Using Molinspiration server the ADME properties of the selected ligands was determined [19-21]. Molinspiration offers calculation of various molecular properties needed in QSAR and drug design. Molinspiration predicts physically significant descriptors and pharmaceutically relevant properties of molecules. Molinspiration supports cheminformatics for calculation of important molecular properties (logP, polar surface area, number of hydrogen bond donors and acceptors and others), as well as prediction of bioactivity score for the most important drug targets [19,20,21].

Results & Discussion

■ Homology modelling and model verification

The amino acid sequences of AMPA receptor was downloaded from NCBI (**Table 1**). Their homologous templates were selected by BLAST (**Table 1**).

The amino acid sequences of the receptors along with their homologous templates were submitted to modeller software for the generation of the 3D structures of the receptors using the principles of homology modeling [17]. Modeller generated five models for each receptor. The 3D models generated by modeler of AMPA (**Table 2**) are

submitted to Rampage Ramachandran Plot server for model verification [18]. The best 3d AMPA (Figures 1 and 2) model is selected.

■ Structure-based pharmacophore

Pharmacophore sites were created in the AMPA receptor (model 3) using the known ligands viz., Oxiracetam [22,23] and Piracetam [24]. The above ligands are established ligands for AMPA receptor. Based on the pharmacophore site information (Figure 3) in the receptor, the unknown ligands in Table 3 were screened.

As per Structure-Based Pharmacophore results phytocompound in Table 3 were selected as

the best fitted ligands (Table 3) and the further docking studies (Figure 3) were done using these phyto-compounds.

■ Molecular docking

AMPA receptor (model 3) was docked with the phytocompound using Docking server. It was seen that AMPA receptor docks with the phytocompounds in Table 4 (Figure 4).

■ ADME screening

Molinspiration generated the following output (Table 5) for the phytocompounds selected in Table 4.

Table 1: AMPA receptor with its GenBank accession number and homologous templates.

Receptor	Accession Number	Homologous templates
AMPA	AAI50210.1	5IDEB 4UQQA 4UQ6A

Table 2: Ramachandran plot analysis of AMPA receptor’s modeler generated models.

	Number of residues in favoured region	Number of residues in allowed region	Number of residues in outlier region	
Model 1	391 (90.7%)	32 (7.4%)	8 (1.9%)	
Model 2	393 (91.2%)	23 (5.3%)	15 (3.5%)	
Model 3	393 (91.2%)	28 (6.5%)	10 (2.3%)	Selected
Model 4	395 (91.6%)	23 (5.3%)	13(3.0%)	
Model 5	382 (88.6%)	37 (8.6%)	12 (2.8%)	

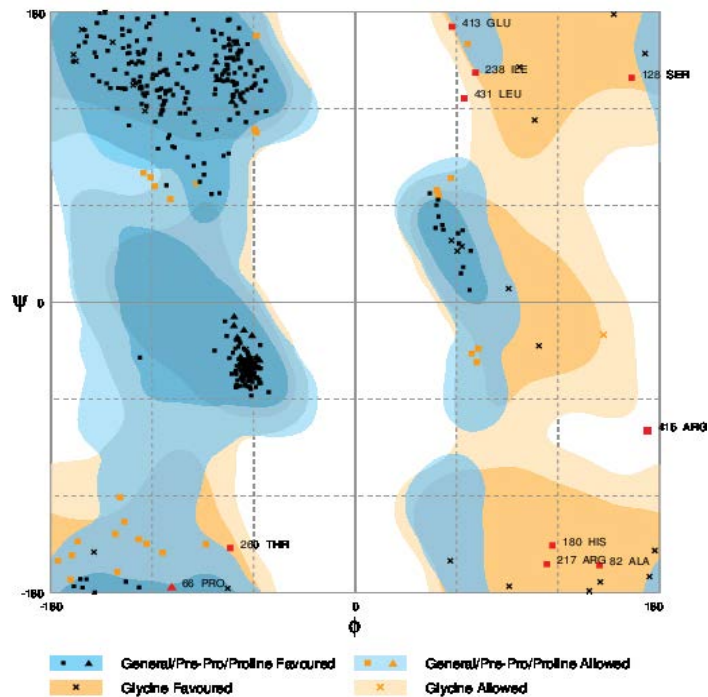


Figure 1: Ramachandran plot analysis of AMPA receptor model 3.

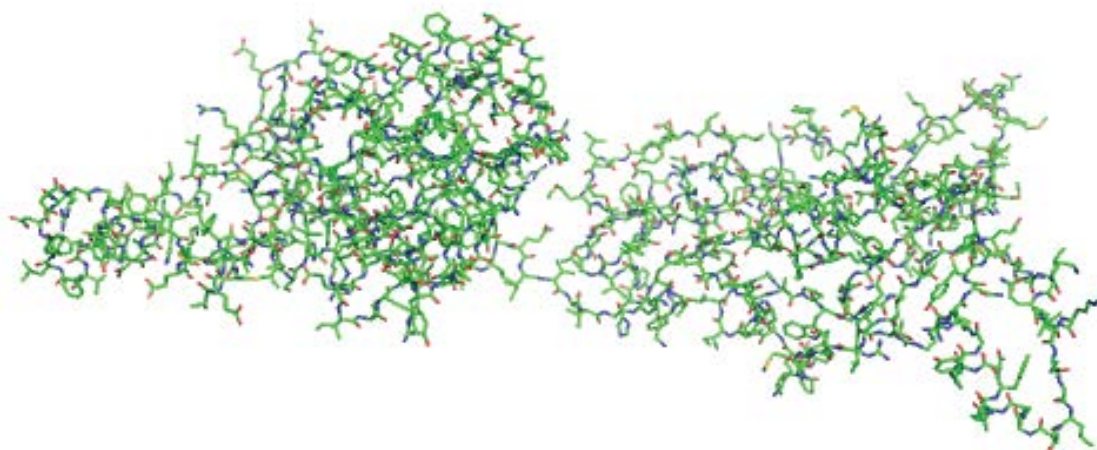


Figure 2: 3D structure of AMPA receptor model 3.

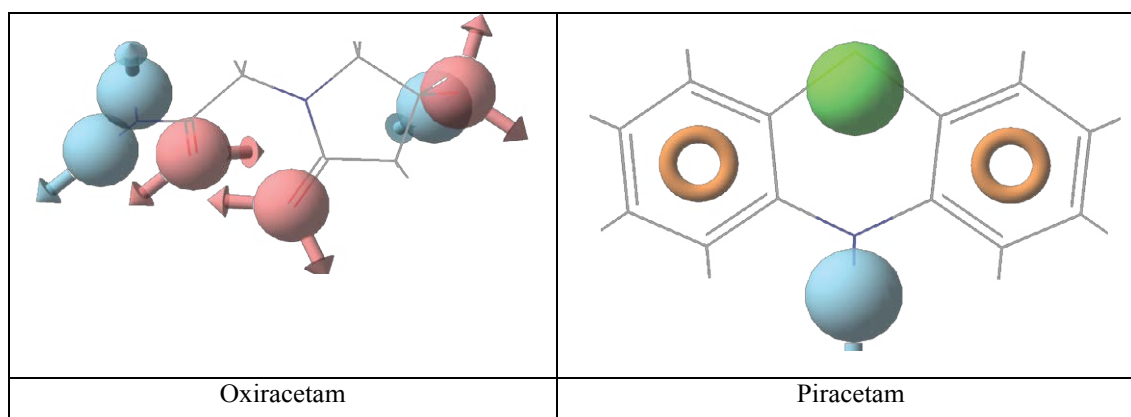


Figure 3: Pharmacophore features of oxiracetam and piracetam.

Table 3: Pharmacophore analysis of phytocompounds.			
Sl. No.	Phyto-Compound under study	Plant Name	Fitness score
Oxiracetam			
1	20-Oxodotriacontanol.1	<i>Convolvulus pluricaulis</i>	1.204752
2	1-Deoxynojirimycin.1	<i>Morus alba</i>	1.075382
3	Bacopaside II.1	<i>Bacopa monnieri</i>	1.040053
4	beta-Glucogallin.1	<i>Phyllanthus emblica</i>	1.021548
5	Deacylgymnemic Acid.1	<i>Gymnema sylvestre</i>	1.033705
6	Eclalbasaponin I.1	<i>Eclipta alba</i>	1.137095
7	Glycyrrhizin ammonical hydrate.1	<i>Glycyrrhiza glabra</i>	1.182755
8	Gymnemagenin.1	<i>Gymnema sylvestre</i>	0.802587
9	Negundoside.1	<i>Vitex negundo</i>	0.963057
10	Picroside I.1	<i>Picrorhiza kurrooa</i>	1.351833
11	Picroside II.1	<i>Picrorhiza kurrooa</i>	1.186592
12	Quercetin dihydrate.1	<i>Azadirachta indica</i>	1.004929
13	Rutin.1	<i>Ruta graveolens</i>	1.178817
14	Trigoneoside IVA.1	<i>Trigonella foenum-graecum</i>	1.0429
Piracetam			

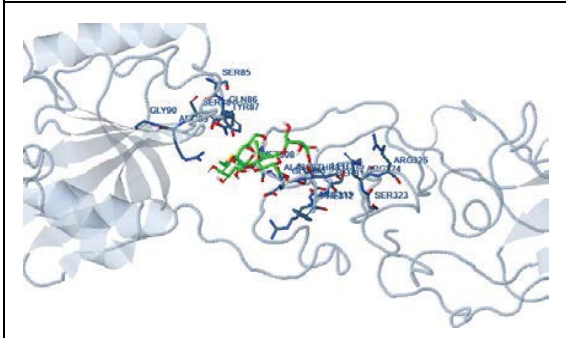
15	vicine.1	<i>Momordica charantia</i>	1.351266
16	Agnuside.1	<i>Vitex negundo</i>	1.315252
17	arjunetin.1	<i>Terminalia arjuna</i>	1.193699
18	arjungenin.1	<i>Terminalia arjuna</i>	0.979138
19	Asiatic acid.1	<i>Centella asiatica</i>	0.882453
20	Bacopaside A.1	<i>Bacopa monnieri</i>	1.36562
21	Catechin 5-O-gallate.1	<i>Acacia nilotica</i>	1.099072
22	chebulagic acid.1	<i>Terminalia chebula</i>	1.077451
23	chebulinic acid.1	<i>Terminalia chebula</i>	1.048981
24	Chlorogenic Acid.1	<i>Coffea Arabica</i>	1.25777
25	D-Pinitol.1	<i>Sutherlandia frutescens/</i> <i>Bougainvillea spectabilis</i>	1.599359
26	Epicatechin-3-gallate.1	Tea	1.098369
27	Epigallocatechin 3-gallate.1	Tea	1.110839
28	Gallic Acid.1	<i>Phyllanthus emblica</i>	1.235741

N.B.- Phyto-compounds with their plant source used in this work
(Source: Natural Remedies, Bangalore, India & Satsang Bhesaj Udyan, Deoghar, India)

Table 4: Docking results.

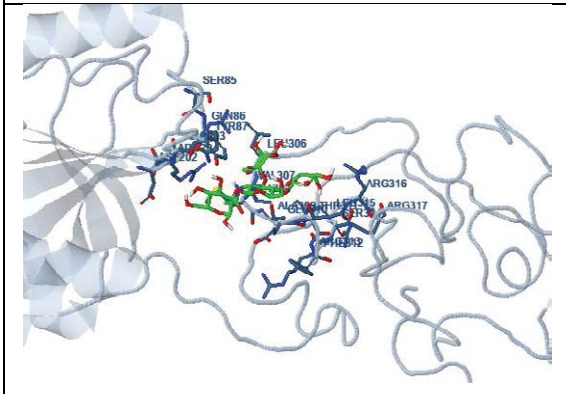
Ligand Name	Binding Energy	No. of Interactions	Dock	
20-Oxodotriacontanol	-5.00	20	Yes	
1-Deoxynojirimycin	-5.52	24	Yes	
Bacopaside II	-8.32	20	Yes	SELECTED
beta-Glucogallin	-3.18	20	Yes	
Deacylgymnemic Acid	-7.56	23	Yes	
Eclalbasaponin I	-8.24	25	Yes	SELECTED
Glycyrrhizin ammonical hydrate	-5.51	16	Yes	
Gymnemagenin	-6.90	15	Yes	
Negundoside	-5.93	20	Yes	
Picroside I	-5.93	20	Yes	
Picroside II	-6.51	30	Yes	
Quercetin dihydrate	-6.10	27	Yes	SELECTED
Rutin	-4.79	21	Yes	
Trigoneoside IVA	-5.30	23	Yes	
Vicine	-4.69	18	Yes	
Agnuside	-5.56	21	Yes	
arjunetin	-8.26	22	Yes	SELECTED
arjungenin	-6.59	23	Yes	
Asiatic acid	-7.95	23	Yes	SELECTED
Bacopaside A	-5.88	15	Yes	
Catechin 5-O-gallate	-5.39	24	Yes	
chebulagic acid	-5.86	24	Yes	
Gallic Acid	-4.01	15	Yes	
chebulinic acid	-6.69	19	Yes	
Epigallocatechin 3-gallate	-5.14	24	Yes	
Chlorogenic Acid	-4.34	9	Yes	
Epicatechin-3-gallate	-6.36	36	Yes	SELECTED
D-Pinitol	-4.26	8	Yes	

20-Oxodotriacontanol



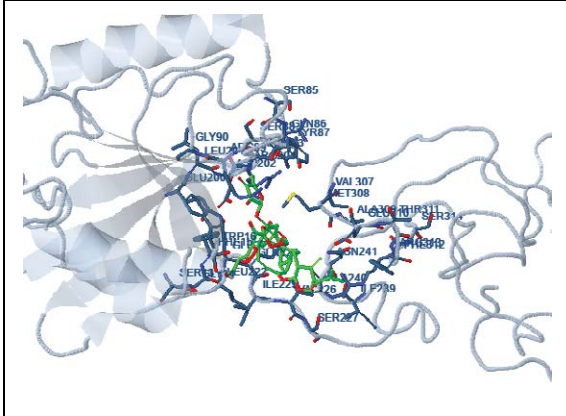
Interaction Table			
hydrogen bonds	polar	hydrophobic	other
O10 (10) - THR311 [2.7]	O5 (9) - GLN86 [2.8]	C16 (37) - TYR87 [2.4] (CD1, CE1)	O15 (15) - TYR87 [2.4] (CD1, CE1)
O14 (14) - THR311 [3.4]	O13 (13) - ARG89 [3.7] (NH1)		O1 (1) - GLU310 [3.4] (CO)
O11 (11) - THR311 [2.7]	O10 (10) - GLU310 [2.9] (CO2)		O10 (10) - GLU310 [3.4] (CO, CO)
H3 (9) - GLU310 [3.7]	O1 (1) - THR311 [4.4] (OO1)		C2 (23) - GLU310 [3.7] (CO, CO2)
H7 (54) - THR311 [3.4]			C10 (37) - GLU310 [3.4] (CO)
H4 (9) - THR311 [3.4]			C15 (36) - THR311 [3.4] (OO1)
H3 (8) - PHE312 [3.4] (OO1)			C12 (33) - THR311 [3.4] (OO1)
H7 (54) - ARG324 [3.7] (OO1)			

1-Deoxynojirimycin



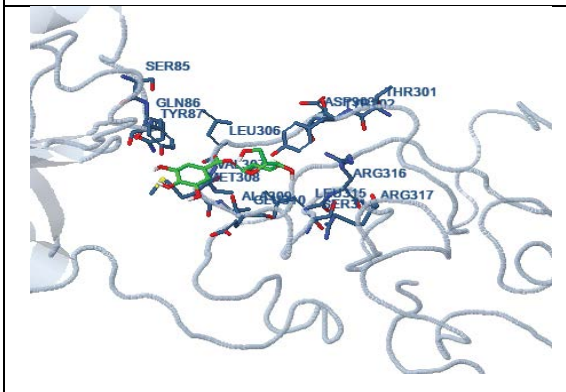
Interaction Table			
hydrogen bonds	polar	hydrophobic	other
O9 (8) - THR311 [2.8] (CA, OO1)	H13 (8) - GLN86 [3.7] (NE2)	C26 (47) - MET308 [2.2] (CA, CO)	O11 (11) - GLN86 [3.3] (CO)
O13 (13) - ARG316 [2.4] (CA, NH1, NH2)	O14 (14) - GLN86 [3.8] (NE2)	C24 (45) - MET308 [3.4] (CO)	H4 (9) - GLN86 [3.4] (CO, CO)
H2 (49) - THR311 [3.7]	O17 (17) - ARG203 [3.4] (NH1)		C15 (36) - GLN86 [3.4] (NE2)
H6 (53) - ARG316 [3.4] (NH1, NH2)	H9 (9) - GLU310 [3.3] (OE1)		O18 (18) - ALA309 [3.4] (CE)
	O10 (10) - THR311 [3.4] (OO1)		H11 (50) - ALA309 [3.4] (CE)
	O15 (15) - ARG316 [2.8] (NH1)		C4 (25) - GLU310 [3.4] (CO)
			C10 (37) - GLU310 [3.4] (CO)
			H9 (9) - GLU310 [3.4] (CO)
			C11 (32) - THR311 [3.7] (OO1)
			C10 (37) - THR311 [2.4] (OO1)
			C16 (37) - ARG316 [3.4] (NH1)
			C14 (34) - ARG316 [3.4] (NH1)

Bacopaside II



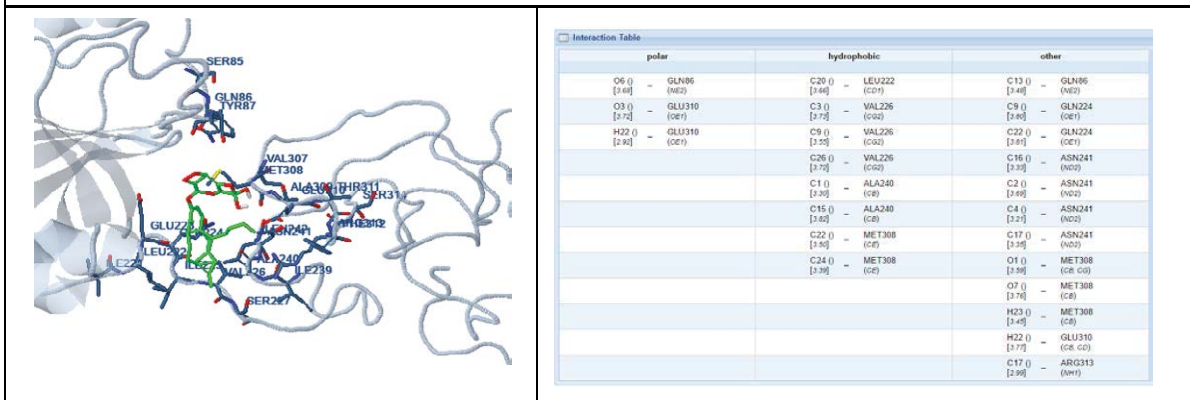
Interaction Table			
polar	hydrophobic	pi-pi	other
O8 (1) - ARG89 [3.4] (CO)	C11 (1) - PHE15 [3.4] (CO)	C20 (1) - PHE15 [3.4] (CO)	O9 (1) - PHE15 [3.4] (CO)
	C23 (1) - PHE15 [3.3] (CD1, CE1)		C40 (1) - GLN86 [3.8] (OE1)
	C4 (1) - VAL226 [3.4] (CO2)		C12 (1) - GLN224 [3.4] (OE1)
	C2 (1) - ALA240 [3.4] (CO)		O6 (1) - ALA240 [3.4] (CO)
	C33 (1) - ALA240 [2.4] (CO)		C42 (1) - GLU310 [3.4] (CO, CE1, OE1)
	C29 (1) - MET308 [3.7] (CE)		C39 (1) - GLU310 [3.3] (OE1)
			C36 (1) - GLU310 [3.4] (OE1)
			C43 (1) - ARG313 [3.4] (CA, NH1, NH2)
			C14 (1) - ARG313 [3.4] (NH1)
			C21 (1) - ARG313 [3.4] (NH1)
			C33 (1) - ARG313 [3.4] (NH1, NH2)
			C39 (1) - ARG313 [3.7] (NH1)

Beta-Glucogallin

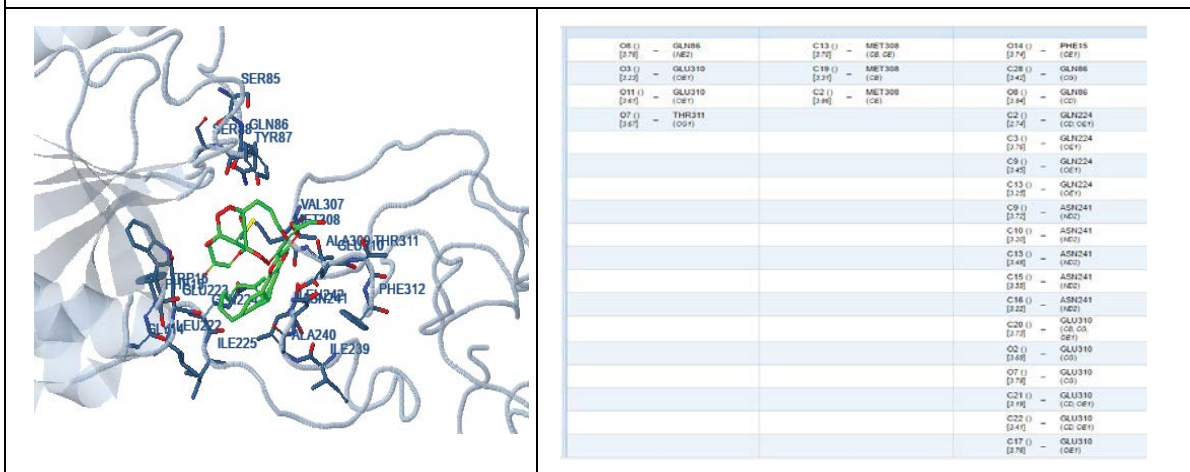


Interaction Table			
polar	hydrophobic	cation-pi	other
O10 (1) - GLN86 [3.7] (NE2)	C12 (1) - MET308 [3.7] (CO)	H2 (1) - TYR302 [2.8] (CE1, CE2, CZ)	C12 (1) - GLN86 [3.7] (NE2)
H7 (1) - GLN86 [3.7] (NE2)	C9 (1) - MET308 [2.4] (CO)		O3 (1) - TYR302 [3.7] (CE1, CZ)
O9 (1) - GLN86 [3.1] (NE2)			O9 (1) - MET308 [3.7] (CO)
H6 (1) - GLN86 [2.4] (NE2)			O5 (1) - ALA309 [3.4] (CE)
O5 (1) - TYR302 [3.4] (OH)			H3 (1) - ALA309 [3.4] (CE)
H3 (1) - TYR302 [3.4] (OH)			H3 (1) - LEU315 [3.4] (CD1, CO)
O3 (1) - TYR302 [3.3] (OH)			O6 (1) - LEU315 [3.7] (CO)
H2 (1) - TYR302 [3.4] (OH)			
O2 (1) - ARG316 [3.4] (NH1)			
H1 (1) - ARG316 [3.7] (NH1)			

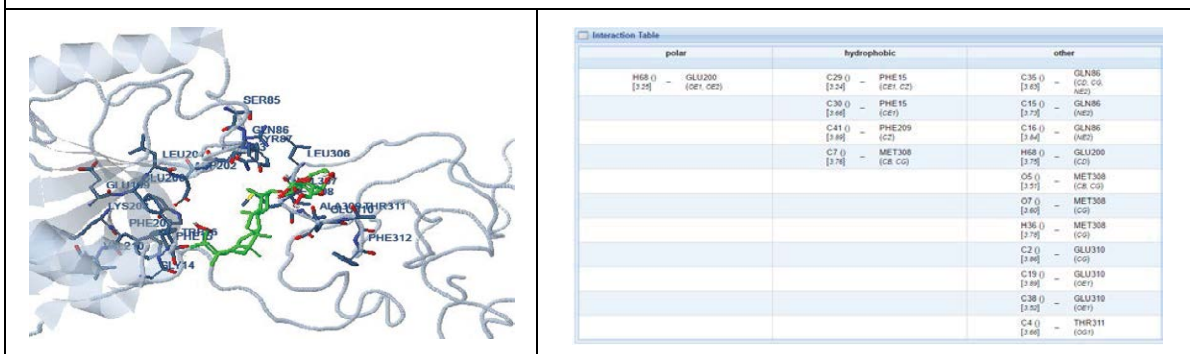
Deacylgymnemic Acid



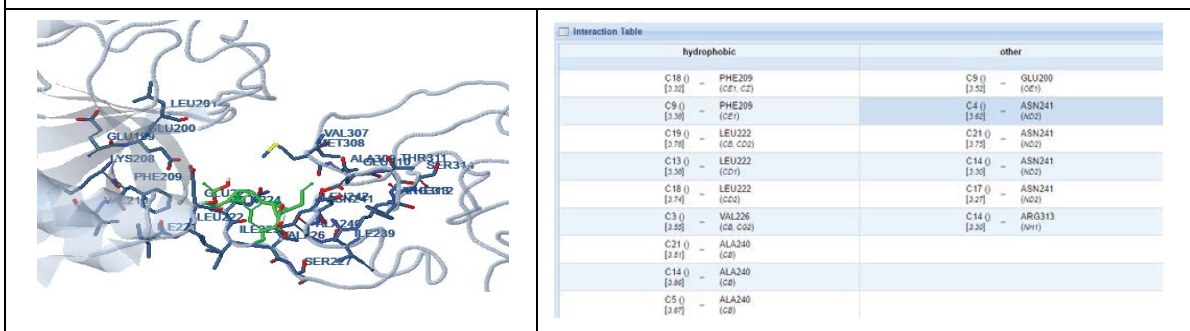
Eclalbasaponin I



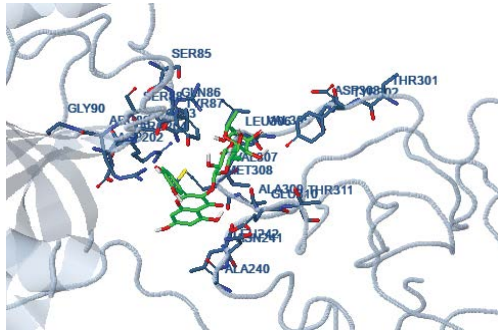
Glycyrrhizin Ammonical Hydrate



Gymnemenin

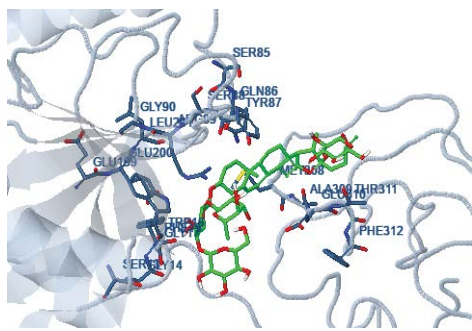


Rutin



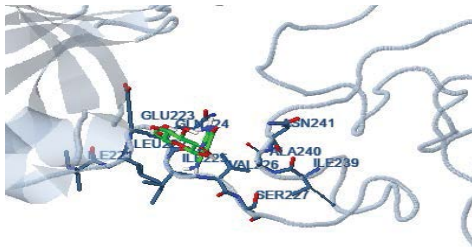
polar		hydrophobic		other	
H10 ([2.6])	- ARG85 (NH1)	C8 ([2.3])	- LEU306 (C2, C22)	O7 ([2.2])	- GLN86 (C8)
O10 ([2.6])	- ARG203 (NH1)	C15 ([2.5])	- MET300 (C8)	H3 ([2.4])	- GLN86 (C2)
H6 ([2.2])	- ARG203 (NH1)	C23 ([2.7])	- MET300 (C8)	C26 ([2.3])	- GLN86 (C2, NE2)
O13 ([2.5])	- ASN241 (ND2)			O22 ([2.1])	- GLN86 (NE2)
O9 ([2.4])	- TYR302 (OH)			C11 ([2.1])	- ARG203 (NH1)
O12 ([2.7])	- GLU310 (OE1)			C8 ([2.5])	- ARG203 (NH1)
				C12 ([2.2])	- ARG203 (NH1)
				O18 ([2.2])	- LEU306 (C2)
				H6 ([2.7])	- LEU306 (C2)
				O13 ([2.4])	- MET300 (C8)
				H7 ([2.1])	- MET300 (C2)
				O12 ([2.7])	- GLU310 (C8)

Trigoneoside IVA



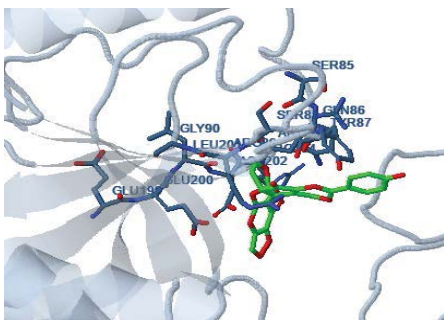
polar		hydrophobic		cation-pi		other	
O7 ([2.7])	- TRP16 (NH1)	C32 ([2.4])	- PHE15 (C2, OE1)	H2 ([2.8])	- PHE15 (C2, OE1)	O7 ([2.1])	- PHE15 (C2, OE1)
O6 ([2.3])	- ARG89 (NH1)	C30 ([2.7])	- PHE15 (C2)	H3 ([2.8])	- PHE15 (C2, OE1)	O4 ([2.8])	- PHE15 (C2)
O10 ([2.7])	- ARG89 (NH1)			H2 ([2.8])	- TRP16 (CO1)	O11 ([2.7])	- PHE15 (C2)
H5 ([2.7])	- ARG89 (NH1)					O7 ([2.2])	- TRP16 (CO1)
O19 ([2.3])	- ARG89 (NH2)					C6 ([2.4])	- GLN86 (C2, C8, NE2)
						C8 ([2.6])	- ARG203 (C2)
						C10 ([2.1])	- GLN86 (C2)
						C16 ([2.2])	- GLN86 (C2, C8, NE2)
						C36 ([2.3])	- ARG89 (NH1)
						C37 ([2.5])	- ARG89 (NH1)
						C20 ([2.1])	- THR311 (CO1)
						C24 ([2.1])	- THR311 (OE1)
						C27 ([2.1])	- THR311 (CO1)

Vicine



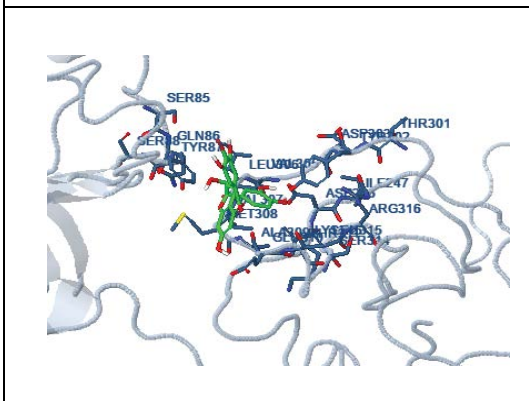
hydrogen bonds		polar		hydrophobic		other	
N4 ([2.7])	- GLN224 (C2, CO1, OE1)	H8 ([2.1])	- GLN224 (OE1)	C6 ([2.4])	- LEU222 (C8, CO2)	H6 ([2.3])	- LEU222 (C8, CO1)
N1 ([2.6])	- GLN224 (C2, CO1, OE1)	H9 ([2.5])	- GLN224 (OE1)	C4 ([1.1])	- LEU222 (CO2)	N3 ([2.8])	- LEU222 (CO1)
N2 ([2.4])	- ALA240 (C)			C10 ([2.5])	- VAL226 (C2)	H7 ([2.2])	- LEU222 (CO1)
						H8 ([2.1])	- GLN224 (C2, CO1, OE1)
						H9 ([2.5])	- GLN224 (C2, CO1, OE1)
						H6 ([2.3])	- ILE225 (C2)
						N1 ([2.2])	- VAL226 (C8, CO2)
						H5 ([2.4])	- VAL226 (C8, CO2)
						N4 ([2.7])	- VAL226 (CO2)
						H9 ([2.5])	- VAL226 (CO2)

Agnuside



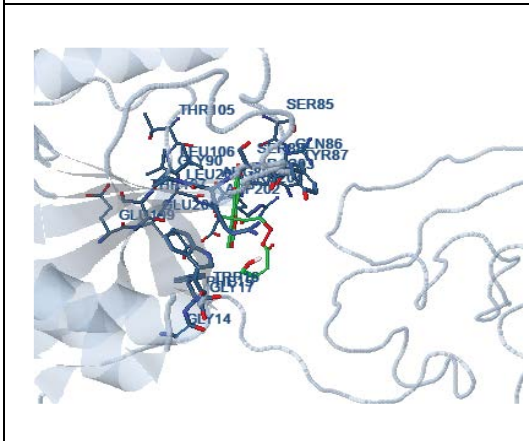
polar		other	
O2 ([2.3])	- GLN86 (NE1, OE1)	C12 ([2.5])	- GLN86 (C2)
O4 ([2.7])	- GLN86 (NE2)	C15 ([2.6])	- GLN86 (C2)
O3 ([2.7])	- ARG89 (OH, NH1)	O7 ([2.6])	- GLN86 (C2)
O6 ([2.2])	- GLU200 (OE2)	C4 ([2.6])	- GLN86 (C2, NE2)
O5 ([2.2])	- ASP202 (CO1)	O2 ([2.4])	- GLN86 (C2)
O19 ([2.7])	- ASP202 (CO1)	C8 ([2.5])	- GLN86 (C2, NE2)
O8 ([2.4])	- ASP202 (CO1)	C10 ([2.1])	- GLN86 (CO1)
O6 ([2.3])	- ASP202 (CO1)	O6 ([2.1])	- GLU200 (C2)
		C16 ([2.4])	- ASP202 (C2, CO1)
		C14 ([2.4])	- ASP202 (C2, CO1)
		C9 ([2.7])	- ASP202 (CO1)
		C13 ([2.1])	- ASP202 (CO1)
		C11 ([2.8])	- ASP202 (CO1)

Catechin 5-O-Gallate



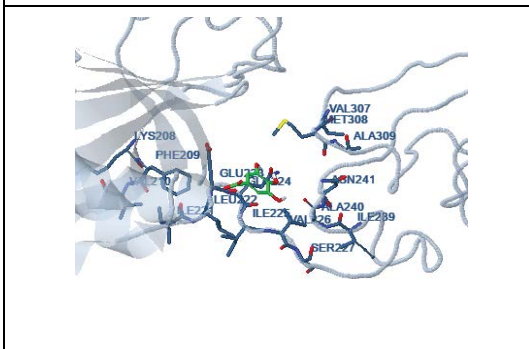
hydrogen bonds		polar		cation-pi		other	
O5 ([2.7])	- TYR302 (cz, oh)	O2 ([3.4])	- GLN86 (ne2)	H5 ([3.4])	- TYR87 (ce)	C22 ([3.4])	- GLN86 (ce)
O6 ([2.3])	- TYR302 (ce, cz, oh)	H1 ([3.3])	- GLN86 (ne2)	H3 ([2.7])	- TYR302 (ce, ce2, cz)	O10 ([3.6])	- GLN86 (ce)
		H3 ([1.8])	- TYR302 (oh)	H4 ([1.7])	- TYR302 (ce, ce2, cz)	H7 ([3.2])	- GLN86 (ce)
		H4 ([2.0])	- TYR302 (oh)			O8 ([3.6])	- TYR87 (ce)
		O4 ([2.4])	- GLU310 (oe1)			C13 ([2.7])	- TYR302 (oh)
			- GLU316 (oe1)			C15 ([2.7])	- TYR302 (oh)
						O5 ([2.7])	- LEU306 (co2)
						O1 ([3.6])	- MET308 (ce, co)
						O4 ([2.4])	- GLU310 (ce, co, co2)
						H2 ([2.3])	- GLU310 (ce, co, co2)
						C11 ([1.5])	- GLU310 (co)
						O6 ([3.4])	- LEU315 (co1)
						H4 ([2.5])	- LEU315 (co1)

Chebolic Acid



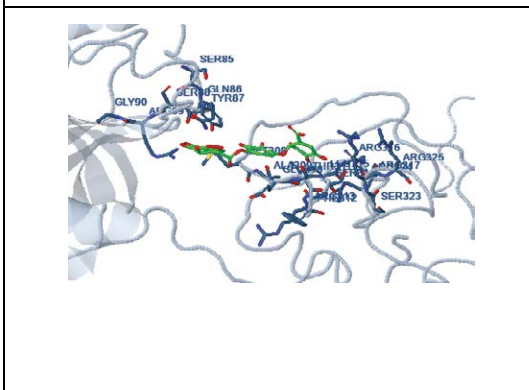
polar		hydrophobic		other	
O3 ([2.2])	- TRP16 (ne1)	C6 ([2.4])	- PHE15 (co1)	C8 ([])	- GLN86 (ce1)
O5 ([3.4])	- GLN86 (oe1)			C11 ([])	- GLN86 (oe1)
O7 ([3.4])	- GLN86 (oe1)			C14 ([])	- GLN86 (oe1)
O6 ([])	- ARG89 (ce)			C10 ([])	- ARG89 (ce)
O8 ([])	- ARG89 (co, co, co)			O5 ([])	- LEU106 (co2)
O3 ([])	- ARG89 (co, cz, ne, ne1)			C3 ([])	- GLU200 (oe2)
H12 ([])	- ARG89 (co, cz, ne1)			C5 ([])	- GLU200 (oe2)
O11 ([])	- ARG89 (ne1)			C12 ([])	- GLU306 (oe2)
O1 ([])	- GLU200 (oe2)			H1 ([])	- ASP202 (co)
H1 ([])	- GLU200 (oe2)			C5 ([])	- ASP202 (co1)
O2 ([])	- ASP202 (co1)				
O1 ([])	- ASP202 (co1)				
H1 ([])	- ASP202 (co1)				

Galic Acid



hydrogen bonds		polar		other	
O5 ([3.3])	- GLU223 (n)	O2 ([3.0])	- GLN224 (oe1)	O5 ([3.7])	- PHE209 (ce1)
		H2 ([2.5])	- GLN224 (oe1)	O6 ([3.4])	- LEU222 (ce, co2)
		O1 ([2.4])	- GLN224 (oe1)		
		H1 ([2.2])	- GLN224 (oe1)	H2 ([])	- GLN224 (ce, co, co2)
				H1 ([])	- GLN224 (ce, co, co2)
				O1 ([])	- GLN224 (co)
				H3 ([])	- VAL226 (ce, co2)
				O1 ([])	- VAL226 (co2)
				H3 ([])	- ALA240 (ce)
				O2 ([])	- MET308 (ce)

Chebulinic Acid



hydrogen bonds		polar		other	
O5 ([2.3])	- ARG89 (ne1)	O11 ([2.1])	- GLN86 (ne, oe1)	C15 ([])	- GLN86 (co, co, ne, oe1)
		O2 ([2.2])	- ARG89 (ne1)	C10 ([])	- GLN86 (co, co, co2)
		O6 ([])	- THR311 (oe1)	O11 ([])	- GLN86 (co)
		O12 ([])	- SER314 (co)	O5 ([])	- TYR87 (ce, ce1, ce2)
		O12 ([])	- ARG316 (ne2)	H3 ([])	- TYR87 (ce, ce1, ce2)
		O12 ([])	- ARG324 (co)		
				C6 ([])	- ARG89 (ne1)
				C11 ([])	- GLU310 (co)
				C23 ([])	- GLU310 (co)
				C23 ([])	- THR311 (co1)
				C12 ([])	- THR311 (oe1)
				C20 ([])	- THR311 (oe1)
				O12 ([])	- SER314 (ce)

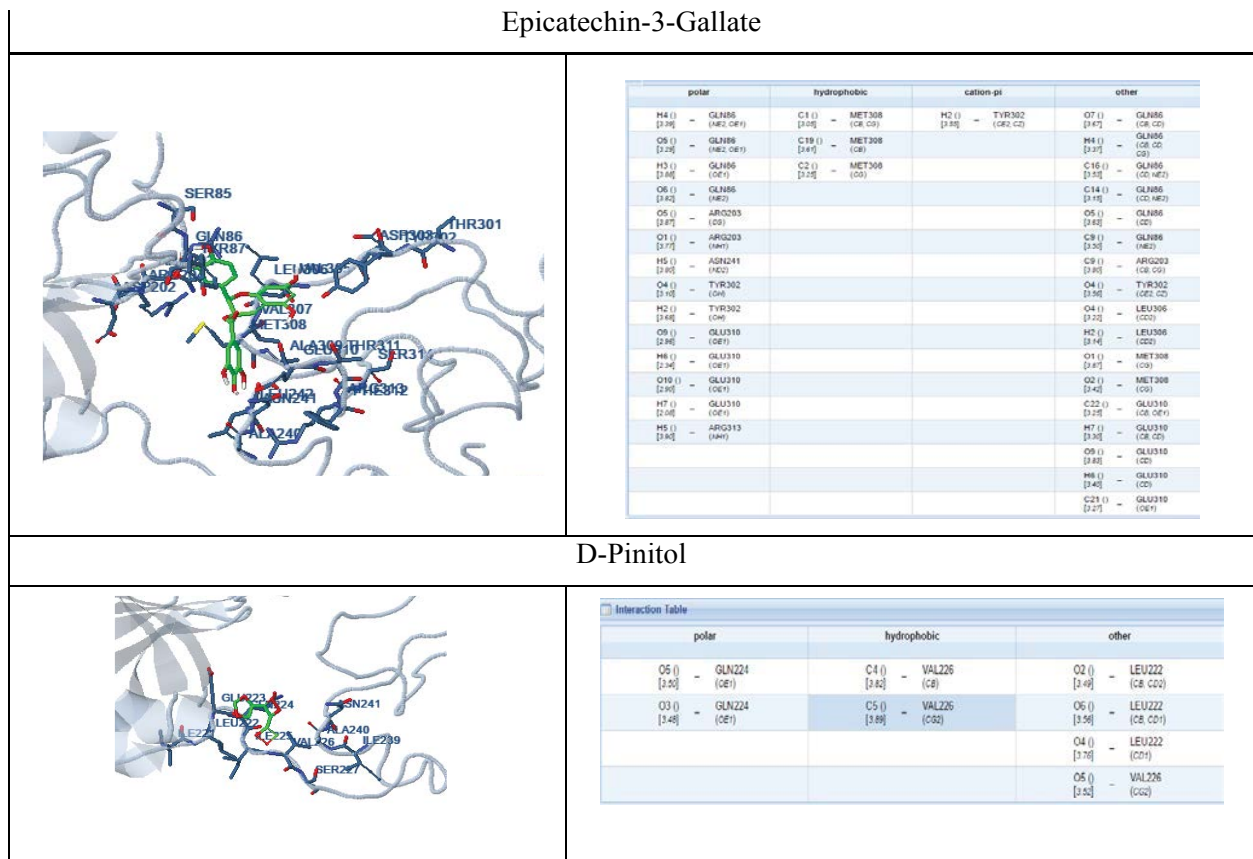


Figure 4: Docking studies of phytochemicals with AMPA receptor with the interacting amino acids.

Table 5: ADME studies.

	miLogP	TPSA	natoms	MW	nON	nOHNH	nrotb	volume	nviolations
Bacopaside II	2.36	276.15	65	929.11	18	10	10	847.65	<u>3</u>
Eclalbasaponin I	2.40	236.06	56	796.99	14	9	7	743.43	<u>3</u>
Quercetin dihydrate	1.68	131.35	22	302.24	7	5	1	240.08	<u>0</u>
arjunetin	2.93	177.13	46	650.85	10	7	5	619.56	<u>2</u>
Asiatic acid	4.70	97.98	35	488.71	5	4	2	487.79	<u>0</u>
Epicatechin-3-gallate	2.54	177.13	32	442.38	10	7	4	359.55	<u>1</u>

Legends: LogP: (octanol/water partition coefficient); TPSA: Molecular Polar Surface Area; natoms: number of atoms; MW: Molecular weight; nON: Number of ON; nOHNH: number of OHNH; volume: Molecular Volume, nrotb: Number of Rotatable Bonds; nviolations: number of violations

Phytochemicals quercetin dihydrate and Asiatic acid were selected as per ADME analysis.

Conclusion

As per Rampage Ramachandran Plot analysis, Model 3 of AMPA receptor is selected as the best model. Further, virtual screening followed by ADME studies it is seen that phytochemicals Quercetin dihydrate from *Azadirachta indica* and Asiatic acid from *Centella asiatica* can be successfully used as ligands for AMPA receptor.

Further in-vitro receptor binding studies are being performed on the above selected receptor with the selected phytochemicals to establish the efficacy of Quercetin dihydrate and Asiatic acid in treating Alzheimer’s disease.

Acknowledgement

This work forms a part of SERB-NPDF for Preenon Bagchi, author reference number PDF/2015/000047.

References

1. Bagchi P, Anuradha M, Kar A. Ayur-informatics: Establishing an ayurvedic medication for Parkinson's disorder. *IJACEBS* 4(1), 21-25 (2017).
2. Bagchi P, Anuradha M, Kar A. Pharmacophore modeling & docking studies of SNCA receptor with some active phytocompounds from selected ayurvedic medicinal plants known for their CNS activity. Under press with Springer AISC series.
3. Bagchi P, Somashekhar R, Kar A. Scope of some Indian medicinal plants in the management of a few neuro-degenerative disorders *in silico*: A review. *Int. J. Public. Ment. Health. Neurosci* 2(1), 41-57 (2015).
4. Gore M, Bagchi P, Desai NS. Ayur-informatics: Establishing an *in silico* ayurvedic medication for Alzheimer's disease. *Int. J. Bioinformatics. Res* 2(1), 33-37 (2010).
5. Burns A, Iliffe S. Alzheimer's disease. *BMJ* 338(1), b158 (2009).
6. Mendez MF. Early-onset Alzheimer's disease: Non-amnesic subtypes and type 2 AD. *Arch. Med. Res* 43 (8), 677-685 (2012).
7. Arnáiz E, Almkvist O. Neuropsychological features of mild cognitive impairment and preclinical Alzheimer's disease. *Acta. Neurologica. Scandinavica* 179(1), 34-41 (2003).
8. Gatz M, Reynolds CA, Fratiglioni L, et al. Role of genes and environments for explaining Alzheimer disease. *Arch. Gen. Psychiatry* 63(2), 168-174 (2006).
9. Chang PK, Verbich D, McKinney RA. AMPA receptors as drug targets in neurological disease -Advantages, caveats and future outlook. *Eur. J. Neurosci* 35(12), 1908-1916 (2012).
10. Honore T, Lauridsen J, Krosgaard-Larsen P. The binding of [3H] AMPA, a structural analogue of glutamic acid, to rat brain membranes. *J. Neurochem* 38 (1), 173-178 (2012).
11. Shi SH, Hayashi Y, Petralia RS, et al. Rapid spine delivery and redistribution of AMPA receptors after synaptic NMDA receptor activation. *Science* 284 (5421), 1811-1816 (1999).
12. Mayer ML. Glutamate receptor ion channels. *Curr. Opin. Neurobiol* 15 (3), 282-288 (2005).
13. Sali A, Blundell TL. Comparative protein modelling by satisfaction of spatial restraints. *J. Mol. Biol* 234(1), 779-815 (1993).
14. Laskowski RA, MacArthur MW, Moss DS. Procheck: A program to check the stereochemical quality of protein structures. *J. Appl. Cryst* 26(1), 283-291 (1993).
15. Schrödinger Suite Protein Preparation Guide, SiteMap 2.4; Glide version 5.6, LigPrep 2.4, QikProp 3.3, Schrödinger, LLC, New York, NY (2010).
16. Taha MO, Dahabiyeh LA, Bustanji Y, et al. Combining ligand-based pharmacophore modeling, quantitative structure-activity relationship analysis and *in silico* screening for the discovery of new potent hormone sensitive lipase inhibitors. *J. Med. Chem* 51(1), 6478-6494 (2008).
17. Singh KHD, Kirubakaran P, Nagarajan S, et al. Homology modeling, molecular dynamics, e-pharmacophore mapping and docking study of Chikungunya virus nsP2 protease. *J. Mol. Model* 18(1), 39-51 (2012).
18. Bikadi Z, Hazai E. Application of the PM6 semi-empirical method to modeling proteins enhances docking accuracy of AutoDock. *J. Cheminformatics* 152009.
19. Ertl P, Rohde B, Selzer P. Fast calculation of molecular polar surface area as a sum of fragment-based contributions and its application to the prediction of drug transport properties. *J. Med. Chem* 43(1), 3714-3717 (2000).
20. Lipinski CA, Lombardo F, Dominy BW. Experimental and computational approaches to estimate solubility and permeability in drug discovery and development settings. *Adv. Drug. Deliv. Rev* 23(1), 4-25 (1997).
21. Veber DF, Johnson SR, Cheng HY, et al. Molecular properties that influence the oral bioavailability of drug candidates. *J. Med. Chem* 45(1), 2615-2623 (2002).
22. Xiao P, Staubli U, Kessler M. Selective effects of aniracetam across receptor types and forms of synaptic facilitation in hippocampus. *Hippocampus* 1(4), 373-80 (1991).
23. Copani A, Genazzani AA, Aleppo G, et al. Nootropic drugs positively modulate alpha-amino-3-hydroxy-5-methyl-4-isoxazolepropionic acid-sensitive glutamate receptors in neuronal cultures. *J. Neurochem* 58(4), 1199-1204 (1992).
24. Ahmed AH, Oswald RE. Piracetam defines a new binding site for allosteric modulators of alpha-amino-3-hydroxy-5-methyl-4-isoxazolepropionic acid (AMPA) receptors. *J. Med. Chem* 53(5), 2197-2203 (2010).